Eur. Phys. J. D **35**, 217–224 (2005)
DOI: 10.1140/epjd/e2005-00189-2

THE EUROPEAN PHYSICAL JOURNAL D

Electron capture by HCl trimers: an ab initio study

A. Rauk and D.A. Armstrong[a]

Department of Chemistry, University of Calgary, Calgary, Alberta T2N 1N4, Canada

Received 4 April 2005 / Received in final form 26 May 2005
Published online 19 July 2005 –

Abstract. The structures and energies of three neutrals and four different anions formed by HCl trimers have been examined by theoretical calculations at MP2 and CCSD(T) levels with large basis sets. In order of increasing binding energy for three HCl molecules, the neutrals are: the Y-shaped species, an open chain Z-shaped form and the cyclic C_{3h} form. Dipole bound anion states are possible for both the Z and Y neutrals, but the DBS of the latter is likely to be short lived. The threshold energies for dissociative attachment (DA) of an electron in the reaction: $e^- + (HCl)_3 \rightarrow H^\bullet + Cl(HCl)_2^-$ at the CCSD(T) level are 0.0 and 0.06 eV, respectively for the Y and Z forms. The cyclic species has no dipole moment and does not attach thermal electrons. The structure of the D_{3h} solvated electron (SE) type trimer anion, was also investigated. Although the structure provides for a high electron affinity (0.33 eV relative to the cyclic trimer) it was unstable and rearranged into a $ClH{\cdot}ClH^\bullet HCl^-$ (SE(2+1)) species. The latter has an EA of 0.59 eV. Vertical detachment energies were also found for these structures. The EAs and vertical detachment energies of the four HCl anion species are discussed and compared to the corresponding species of HF.

PACS. 34.80.Ht Dissociation and dissociative attachment by electron impact – 36.40.Jn Reactivity of clusters – 31.15.Ar Ab initio calculations

1 Introduction

The capture of electrons by neutral molecules is of practical importance in the chemistry of the atmosphere, insulating materials, gas discharges, plasmas and irradiated systems. A detailed understanding of electron interactions with small molecular systems is also of importance in the development of theory. In this regard, the interactions of electrons with hydrogen halide (HX) molecules have been a subject of interest for many years [1–3]. The dissociative attachment (DA) process in HX monomers, reaction (1),

$$HX + e^- \rightarrow H^\bullet + X^- \qquad (1)$$

occurs in competition with rotational and vibrational excitation and has been studied extensively [3–6]. The conclusions from experimental and theoretical studies conductedover the past four decades are covered in recent papers [7–9]. HX molecules have also played an important role in the study of electron binding in solvated electron (SE) and dipole bound anion states (DBS) [10–14]. The $(HF)_2^{\bullet -}$ dimer anion is a DBS with an H-bonded $FH{\cdot}FH^{\bullet -}$ structure not very different from the neutral [11, 12]. At least two forms of the $(HF)_3^{\bullet -}$ trimer anion appear to exist [13]: an asymmetric C_s SE species, $FH{\cdot}FH^\bullet HF^-$ (SE(2+1)), and a DBS with a $FH{\cdot}FH{\cdot}FH^{\bullet -}$ Z-shaped geometry, dbe(Z)[1]. Theoretical calculations also predict the dimeric $XH^\bullet HX^-$ SE structures [15,16], those for HCl and HBr being highly stable. Indeed the experimental observation of $(HCl)_2^{\bullet -}$ dimer anion [10] is best attributed to the $ClH^\bullet HCl^-$ SE structure. The only alternative would be a DBS, but the dipole moment of the neutral HCl·HCl dimer is 1.5 D [17] and below the critical value of 2.2 for formation of a stable DBS [18,19]. Secondly coupled cluster level calculations show no evidence of DBS binding on the neutral dimer geometry [20].

Electron interactions are also of importance when HX molecules are present in irradiated systems, where electrons are produced and rapidly thermalised [21–24]. When DA occurs, as in reaction (1) or with HX clusters in reaction (2):

$$(HX)_n + e^- \rightarrow H^\bullet + X^-(HX)_{n-1} \qquad (2)$$

the resulting $H^\bullet$ atom drives the production of hydrogen in reaction (3). This reaction is

$$HX + H^\bullet \rightarrow H_2 + X^\bullet \qquad (3)$$

too slow for HF, but very efficient with the other hydrogen halides. As a result HCl and HBr have been considered as

[a] e-mail: armstron@ucalgary.ca

[1] The nomenclature of reference [13], dbe, has been adopted for the dipole bound electron. For structural representations of the HF (SE(2+1)) and dbe(Z) species the reader is referred to the analogous HCl species depicted below in Figures 6b and 2b, respectively.

scavengers to enhance hydrogen production in reactor systems [25] and these electron driven processes may in future have practical value. Thus the details of the capture process are of interest. The threshold energies for reaction (1) are 0.39 and 0.82 eV in HBr and HCl, respectively [20], and monomer DA is not competitive for thermal electrons ($KE \simeq 0.04$ eV at 298 K). In the case of HBr an ab initio study [26] has shown that the DA threshold is lowered to 0.0 eV in $(HBr)_2$ dimer.

Experimentally the capture rate in the ambient gas is second order in HBr, and, when allowance is made for the equilibrium dimer concentration, the capture by it is observed to be at near the maximum rate for ∼0.04 eV electrons [27,28]. DA is therefore primarily through reaction (2) with $n = 2$. The situation with HCl is much more complex. While the dimer species is undoubtedly involved, coupled cluster level calculations show that the threshold for reaction (2) with $n = 2$ is substantial, 0.21 eV [20], implying that dimer capture would not be efficient. Also experimentally the capture rate in gas mixtures at 0.1 to 2 atmosphere pressure is overall third order [22–24]. Evidence that reaction (2) might occur with clusters of $n \geq 3$ came from a crossed beam experiment in which electron transfers were observed from fast alkali atoms (namely Rb) to $(HCl)_n$ species [29]:

$$Rb + (HCl)_n \rightarrow Rb^+ + H^\bullet + Cl^-\cdot(HCl)_{n-1}. \quad (4)$$

The $Cl^-\cdot(HCl)_{n-1}$ species were identified by mass analysis. More recently the attachment of electrons to HCl clusters at low temperatures was observed by the CRESU technique, and again the $Cl^-\cdot(HCl)_{n-1}$ products were identified by mass spectrometry [30]. However, neither study gave a clear picture of the threshold energy for reaction (3) for different n.

The third order dependence of the electron capture rate implies that trimer species are involved. The purpose of this paper was therefore to determine the structures and energies of anions which could be formed from HCl trimers, and to examine potential energy surfaces for DA reactions in $(HCl)_3$ species. As mentioned above, the trimer anions of HF have already been investigated [13]. In general the HCl species described here are analogous, and comparisons between the two halogen systems are made in the Discussion.

2 Computational details

The procedures used here were similar to those employed in reference [20]. The ab initio calculations were performed with the Gaussian-98 and -03 molecular orbital packages [31,32]. Geometry optimizations and vibrational frequency calculations were carried out at the MP2 level with 6-311+G(3df,2p) basis sets on Cl and aug-cc-pVDZ on H. Vibrational frequencies and zero point energies (ZPEs) were scaled with the scaling factors in reference [33], 0.9496 and 0.9748, respectively. CCSD(T) level [34] single point calculations were carried out on the MP2 geometries of the anions and neutrals. Electron binding energies and electron affinities were obtained from the differences in the CCSD(T)//MP2 energies. These methods have been found to reproduce experimental energies to within a few kJ mol^{-1} in related systems [12,13,20].

The present basis sets are quite large and should suffice for orbitals of normal negative ion species. However, for systems where the electron was free and interacting with the molecular dipole up to four additional diffuse functions were added at atomic positions as stated in the text. The diffuse functions used were the sets of s-, p- and d-type Gaussian functions with exponents 0.005625, 0.001125, 0.000225 and 0.000045, and they were added in this order. When these are present, the number and position has been indicated in the text and tables. Since the energies of the neutral trimers serve as reference zero for the anion systems, it was also necessary to calculate the energies of these neutrals with identical diffuse functions. It should be noted that the geometries of the neutrals are insensitive to the presence of the diffuse functions, though this is often not the case for the anions.

The binding energies (BEs) for HCl trimer formation were calculated from the differences in CCSD(T)//MP2 electronic energies according to the equation: $\Delta E = 3E(HCl) - E(HCl)_3$. Corrections for basis set superposition errors (BSSEs) were made as in reference [35]. They were found to be in the range 6–8 kJ mol^{-1} at both MP2 and CCSD(T) levels. Corrections were also made for the ZPEs. The MP2 potential energy profiles for the stretching of the terminal H–Cl bond in the $(HCl)_3^{\bullet-}$ trimer anions to produce the DA products $H^\bullet + Cl^-(HCl)_2$ were obtained by carrying out MP2 calculations at increasing values of r(Cl–H). The geometry of the remainder of the system was optimized at every step. Similar scans at the CCSD(T) level were not possible. However, CCSD(T) calculations were carried out on the MP2 geometries obtained as above. The Opt = (TS) routine employed in reference [20] could not be used due to the larger size of the systems.

3 Results

The neutral HCl trimer can exist in ring, Z and Y shaped geometries [13,36]. MP2 optimized structures were obtained for all of these. Electron binding to each was then investigated by re-optimizing with an electron attached. A fourth type of negative ion, a symmetrical D_{3h} structure with a centrally located solvated electron (SE) type of structure, was also investigated. The structures of the neutrals are shown in Figure 1, along with that of the dimer from reference [20]. The structures of the anions are presented in Figures 2, 4 and 6. For simplicity the same nomenclature has been adopted for the anions as in reference [13], i.e. dbe(Z) and dbe(Y) for the Z- and Y-shaped $(HCl)_3^{\bullet-}$ dipole bound species and SE(3×1) and SE(2+1) for the D_{3h} and C_s $ClH\cdot ClH^\bullet HCl^-$ SE species, respectively. The MP2 and CCSD(T) electronic energies on the MP2 optimized geometries have been presented in Table 1. The neutrals are discussed in Section 1 and the anions in Sections 2, 3, 4 and 5.

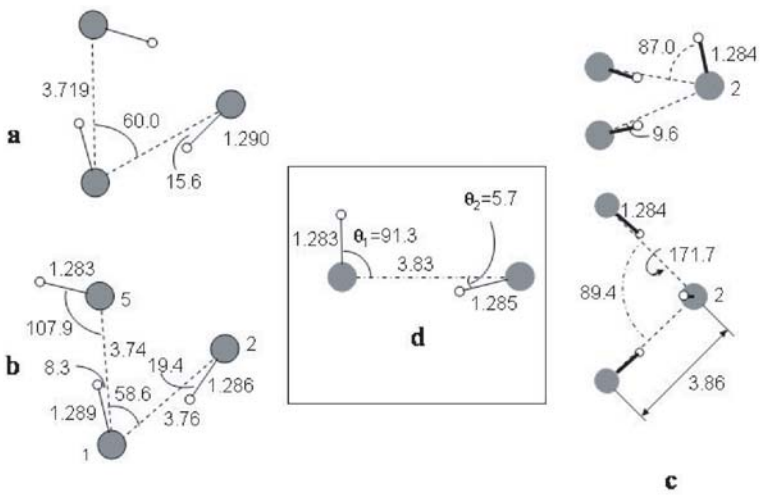

Fig. 1. The three structures of the neutral HCl trimer: (a) cyclic structure with C_{3h} symmetry. (b) Z-shaped with C_s symmetry. (c) Y-shaped with C_s symmetry. (d) The neutral HCl dimer with C_s symmetry. Bond distances in Å, angles in degrees.

Table 1. Electronic energies (in Hartrees) and ZPEs (kJ/mol) of optimized neutrals and anions, and electron affinities (meV).

Geometry	diffuse functions	MP2 energy		CCSD(T) energy		ZPE[a]		EA[b]/mV
		neutral	anion	neutral	anion	neutral	anion	
Cyclic	3*sps* on a central bq	–1380.90339	–1380.90285	–1380.98822	–1380.98768	63.2	62.4	–10
Z	2*spd* on Cl with free H[c]	–1380.90020	–1380.89980	–1380.98536	–1380.98593	61.4	60.9	16
Y								
(a) neutral/DBS	2*spd* on central Cl	–1380.89796	–1380.89818	–1380.98530	–1380.98511	58.8	58.4	43
(b) neutral/valence prod.	1*sp* on central Cl	–1380.89788	–1380.92489	–1380.98341	–1381.00315	58.8	42.1	720
SE(D_{3h})	2*spd* on a central bq	-	–1380.90976	-	–1380.99448	-	47.3[d]	327
SE(C_s)	1*sp* on each of opposed Hs	-	–1380.92119	-	–1381.00672	-	54.0	590

[a] From MP2 frequencies [b] Relative to cyclic neutral for SE structures and to neutrals of similar geometry for Y and Z. [c] See Table 3 for more detail. [d] Two freqs. are imaginary.

3.1 Neutral trimers

The HCl trimer has been studied by experiment [37,38] and theory [36,39]. The global minimum corresponds to a C_{3h} cyclic structure. The geometry obtained here is shown in Figure 1a. The Cl–Cl–H bond angles, and Cl–Cl and H–Cl distances reported in reference [36] from MP2 calculations are: 16.8°, 3.736 Å and 1.282 Å, respectively. These were obtained with a pseudo-potential double-ζ basis set augmented by diffuse *sp* and polarization functions. The density functional methods used in reference [39] gave Cl–Cl 3.630–3.712 Å and H–Cl 1.305–1.307 Å. The present values fall in between these. The experimental value of the separation between HCl centres of gravity is 3.693 Å [38]. Our binding energy at the MP2 level was 13.4 kJ mol^{-1}. This is lower than the MP4(SDTQ) value reported in reference [36] (17.6 kJ mol^{-1}), but similar to that from the MPW1PW91/aug-cc-pVDZ density functional study of reference [39] (13.6 kJ mol^{-1}). The present CCSD(T) value is 8.9 kJ mol^{-1}. There does not appear to be an experimental value. The scaled MP2 frequency for the doubly degenerate H–Cl asymmetric vibration was 2784 cm^{-1}, in good agreement with the experimental band origin (2809.8 cm^{-1}[38]). These comparisons indicate that the present MP2 calculations are adequate to describe the C_{3h} trimer.

The structure of the HCl dimer is shown in Figure 1d, and its relation to the trimers is now examined. While the C_{3h} structure is made from it by completing the ring, the other two trimers are made by adding the third HCl in other ways. These are not as stable, but, as will be shown below, are more likely to play a role in electron capture. The Z structure is of C_s symmetry with one HCl proton rotated ∼180° from the position in the C_{3h} structure. Interestingly there is only a small perturbation of the equilateral triangular arrangement of the 3Cls. The Cl–Cl distances expand slightly from the C_{3h} values, but remain shorter than in the dimer. The H to Cl bond length in the middle HCl is close to that in the cyclic trimer, while those in the pure donor and acceptor HCls closely approximate the corresponding ones in the dimer. The Y shaped trimer (Fig. 1c) has two HCls donating their protons to the central Cl. The H–Cl bond distances and H–Cl–Cl angles here are close to those of the dimer, and the Cl–Cl–Cl angle is close to 90°. The Cl–Cl distances are now longer than in the dimer. The MP2 and CCSD(T) binding energies of the Z and Y forms are listed in Table 2 along with those of the cyclic form. At both levels they become weaker in the series cyclic, Z, Y.

3.2 C_{3h} cyclic anion

The anion form of the C_{3h} neutral was optimized in the absence of diffuse functions, as well as with one set of *sp* functions on each Cl, and with 3 sets of *sp* functions on a

Table 2. Binding energies of trimers (kJ mol^{-1}).

geometry	MP2	CCSD(T)
cyclic	13.4	8.9
C_s Z	8.0	4.8
C_s Y	5.1	3.0

central dummy atom. Without diffuse functions the structure expands (Cl–Cl = 3.98 Å) relative to the neutral, but there is no significant change in the presence of the diffuse functions. Also the frequencies of the anion and neutral are similar. The energy of the anion remained above that of the neutral, even at CCSD(T) level with 3 sets of *sp* functions on a central dummy atom (Tab. 1). In short the electron is unbound and remains in the continuum.

Since each H–Cl in the cyclic trimer is both a proton donor and a proton acceptor, it would be expected that the solvating effect of the additional HCls would not substantially lower the level of the HCl σ^* valence orbitals, as occurs in HX·HX dimers [26,20]. An indication of the level of these orbitals was obtained by calculating the energy of the anion relative to the neutral without additional diffuse functions. This was found to be 0.65 eV, only slightly lower than obtained from a similar calculation on the isolated HCl monomer, 0.72 eV. Thus the effect of solvation in the cyclic C_{3h} geometry is small, and the threshold level for DA will be relatively high. It was not examined here.

3.3 Z shaped anion, dbe(Z)

The geometry of the Z shaped anion in Figure 2 can be compared with that of the corresponding neutral, which is repeated there for comparison. The anion geometry and electron binding were examined by optimizing it with several different sets of diffuse functions. A few results are shown in Table 3. The electron binding energy is with respect to the optimized neutral and has been corrected for ZPEs. The anion system evidently strikes a compromise between becoming linear, which would maximize the dipole moment and give greatest dipole binding of the electron, and maintaining the inherent geometry of the neutral framework. With only 1 set of *sp* functions the Cl–Cl–Cl angle is 101.4° and the neutral framework has the highest dipole moment, but the electron is still unbound. With two sets of *sp* functions the available orbital space increases substantially (see expectation value of the electronic wavefunction, $\langle r^2 \rangle$, in column four), and the system relaxes toward the neutral geometry, the Cl–Cl–Cl angle falling to ∼90°. At this point the electron is bound. Adding another set of *sp* functions causes a further rise in the orbital space, but the Cl–Cl–Cl angle remains near 90° and the binding does not increase. The highest binding energy of 16 meV was obtained with two sets of *spd* functions, and the structure with these is the one in Figure 2b. With the same basis sets the vertical attachment energy on the neutral geometry was 9 meV. As in many DBS systems, the frequencies of the optimized anion are lower than those of the neutral, for example the terminal Cl–H stretch is reduced from 2860 to 2804 cm^{-1}. The

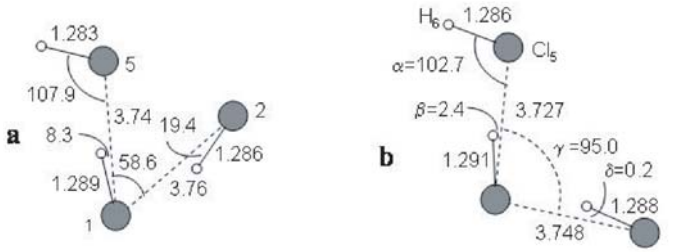

Fig. 2. Comparison of the Z-shaped neutral HCl trimer (a) with the Z-shaped dbe(Z) anion with C_s symmetry (b). Bond distances in Å, angles in degrees.

lower anion frequencies are reflected in a lower ZPE in Table 1.The greatest fractional reduction is in the Cl–Cl–Cl bending mode, which falls from 41 cm^{-1} in the neutral to 10 cm^{-1} in the anion. The presence of the electron clearly modifies the PE curve for this vibration, as expected from the above noted strong interaction with the molecular geometry.

The stability of the Z $(HCl)_3^{\bullet -}$ anion with respect to H atom loss was explored at the MP2 level by scanning the energy as the terminal Cl–H bond was stretched with the geometry of the rest of the system optimized at every step. A similar scan was made for the neutral and the results for it are shown by the dashed line in Figure 3. The dashed horizontal line is the ZPE level of the Cl–H vibration in the neutral. The MP2 energies for the anion are shown by the open circles. These were obtained with up to 3 sets of added diffuse functions on the Cl of the bond being stretched. However, as found in reference [20] (and illustrated for the Y-shaped anion in Fig. 5), the number of these may be reduced without having any effect as the system nears the maximum and crosses into the $H^{\bullet}$ + $Cl{\cdot}(HCl)_2^-$ valence product region, where the spatial extent of the wavefunction becomes smaller. This is dramatically illustrated by the size of the singly occupied molecular orbital (SOMO) of the structures at the curve minimum (r_{HCl} = 1.30 Å) and transition region (r_{HCl} = 1.49 Å), in Figure 3b, both representing the distribution of 1/2 electron. For the purpose of comparison with other systems, an indication of the relative size of the DBS SOMO may be obtained from the difference in the electronic spatial extent $\langle r^2 \rangle$ parameter of the Gaussian calculations of the anion and the neutral on the same geometry. This $\Delta\langle r^2 \rangle$ value for the Z DBS anion is 847 (a.u.)^2.

The PE curve was explored further by doing CCSD(T) calculations on the geometries obtained in the MP2 scan. The results are shown by the filled squares in Figure 3a. The solid line is the best curve through them. As was found in the case of electron attachment to the HCl dimer [20], the MP2 calculations underestimate the anion stability in the dipole bound region and overestimate it in the valence region. The threshold for DA is given by the height of the barrier above the ZPE of the neutral. The value for the CCSD(T) curve is 0.06 eV. In effect this threshold is determined by the position of the avoided crossing between the valence state, with the electron in the σ^* level, and the dbe anion in the PE well of

Table 3. Effect of diffuse functions on geometry and electron binding of Z anion.

diffuse functions on Cl5	dipole moment of neutral on anion geom./D	CCSD(T) EA (relative to Z neutral) /meV	$\langle r^2\rangle$/(au)^2	Cl–Cl–Cl angle/degrees
1 *sp*	3.87	–18	1579	101.4
2 *sp*	3.71	13	1969	93.7
2 *spd*	3.62	16	1977	95.0
3 *sp*	3.57	10	2619	94.4

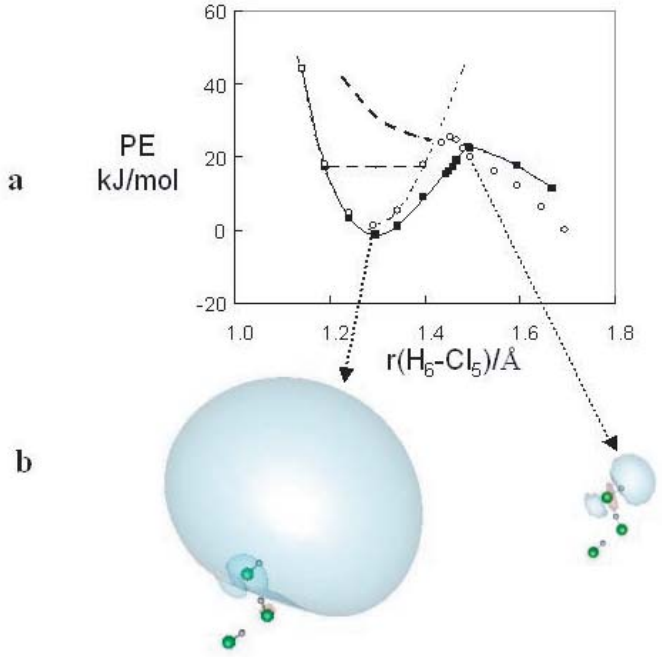

Fig. 3. (a) Potential energy scans for stretching the H_6–Cl_5 bond of the Z-shaped anion (see Fig. 2). MP2 Open circles (○); CCSD(T): closed squares (■) with *sp* functions, heavy dashed line no *sp* functions. (b) Plots of the singly occupied molecular orbital at the indicated points. Each plot illustrates the contour containing 50% of the electron.

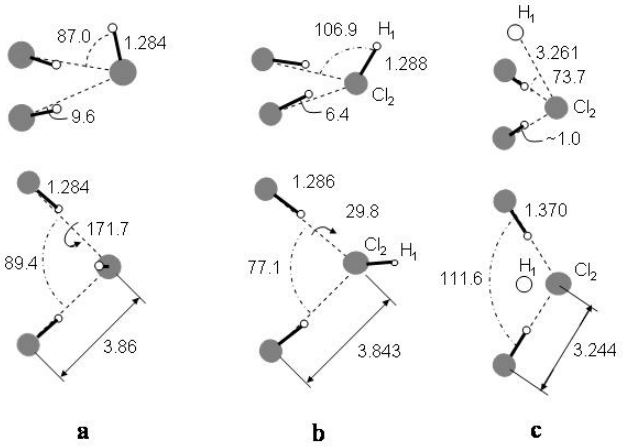

Fig. 4. Comparison of the Y-shaped neutral HCl trimer (a) with the Y-shaped dbe(Y) DBS anion with C_s symmetry (b), and the Y-shaped valence H-atom complex with $ClH{\cdot}Cl{\cdot}HCl^-$ (c). Bond distances in Å, angles in degrees.

the neutral. Within this well the valence state is subject to auto-detachment. The curved heavy dashed line was obtained without diffuse functions, and gives an indication of its energy. At the r_e value of the H–Cl vibration it lies 30 kJ mol^{-1} (0.31 eV) above the neutral of the system. This is significantly reduced from the value in the monomer, and the effects of solvation are much larger than in the cyclic system.

3.4 Y shaped anion, dbe(Y)

The optimized geometries of the Y shaped DBS anion and neutral are compared in Figure 4 (Figs. 4a and 4b). The dipole moment of the neutral at MP2 level was 2.27 D, approximately the critical value for binding an electron (2.2 D, [18,19]). However, fairly small adjustments in the geometry occur in the optimization of the anion geometry and raise it to 3.22 D, thus ensuring DBS formation. Obviously effective are the change in the H–Cl–Cl angle for the terminal H atom from 87.0° to 106.9°, the reduction in the Cl–Cl–Cl angle (89.4° to 77.1°), and the move of the H-bonding protons from below to above the Cl–Cl–Cl plane (Fig.4). In this case the electron was bound in the structure optimized with only 1 set of *sp* functions. The best EA at the CCSD(T)//MP2, 43 meV, was obtained on the structure in Figure 4b, which was optimized with 2 sets of *spd* functions on the central Cl. The same basis sets gave a vertical attachment energy of 20 meV. As with the Z species the terminal Cl–H stretch frequency in the anion is reduced from the value in the neutral, from 2852 cm^{-1} to 2746 cm^{-1}. However, interestingly in this case some of the vibrational frequencies in the anion are *higher* than in the neutral. In particular the weak Cl–Cl–Cl bend frequency increases from 4.8 cm^{-1} to 9.7 cm^{-1}. This is probably related to the need to maintain the high dipole moment. The SOMO of the DBS, representing 1/2 electron, is illustrated in Figure 5b. The $\Delta\langle r^2\rangle$ value (768 (a.u.)^2) is a little smaller than for the Z DBS, reflecting the increase in binding from 16 to 43 meV in Table 1.

As was done for the Z shaped anion, the PE surface for the stretching of the terminal H–Cl bond was examined by scanning the MP2 energy on the Born Oppenheimer surface. The results are shown in Figure 5a, where the dashed curve and dot-dashed horizontal line represent the Cl–H vibrational well in the neutral. The pattern for the MP2 and CCSD(T) points in Figure 5a is similar to that seen in Figure 3a for the Z-shaped anion, with the MP2 energies being higher in the dipole bound region and lower

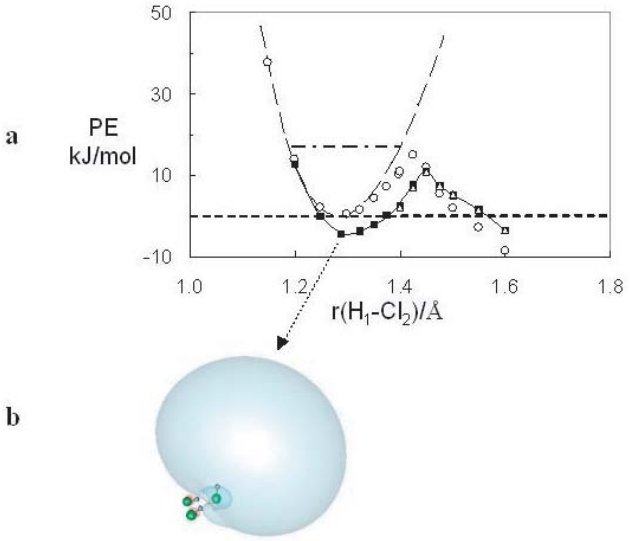

Fig. 5. (a) Potential energy scans for stretching the H_1–Cl_2 bond of the Y-shaped ,anion (see Fig. 4). MP2 Open circles (○); CCSD(T) closed squares (■) 2 sets of *sp* functions on Cl2, open triangles (Δ) one set. (b) Plot of the singly occupied molecular orbital at the indicated point illustrates the contour containing 50% of the electron.

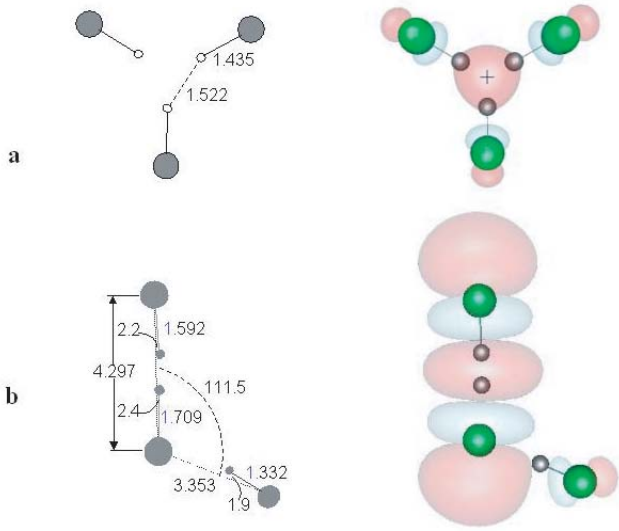

Fig. 6. Plots of the structures and singly occupied molecular orbitals (SOMOs) of the SE anions. (a) SE(3×1) D_{3h} geometry with two imaginary frequencies. (b) SE(2+1) Minimum energy structure. Each SOMO plot illustrates the contour containing 50% of the electron.

in the valence region. Also the barrier to dissociation of the anion at the CCSD(T) level is again lower than at the MP2 level. Both it and the MP2 barrier now fall below the ZPE of the Cl–H vibration in the neutral. Thus the DA threshold for the Y shaped species is 0.0 eV. As a corollary the DBS on this geometry should have only a short lifetime with respect to decomposition to $H^{\bullet}$ + $Cl{\cdot}(HCl)_2^-$. Figure 4c depicts the optimized geometry of the $H^{\bullet}\cdots Cl{\cdot}(HCl)_2^-$ valence product complex, where the H atom remains bound by the ion-induced dipole force. This product lies 720 meV below the Y shaped neutral (Tab. 1). In electron attachment to an isolated Y-shaped trimer it would decompose to $H^{\bullet}$ and $Cl{\cdot}(HCl)_2^-$, since a large part the energy would end up as relative kinetic energy of the fragments.

3.5 SE type anions, SE(3×1) and SE(2+1)

Unlike the anions described above these species have no neutral counterpart, and cannot be formed by a straightforward electron attachment. However, earlier work [16] had shown that a linear dipole opposed ClH...*e*...HCl^- dimeric SE structure was stable, and it was important to determine whether an analogous trimeric HCl D_{3h} SE (SE(3×1)) could also exist. The structure in Figure 6a was obtained by optimizing without diffuse functions and with symmetry constrained to be D_{3h}. Reoptimization with 2 sets of *spd* functions on a central "ghost" atom gave no change. Its energy lies 327 meV below the cyclic neutral (Tab. 1). However, it possesses two imaginary frequencies and is therefore not a local minimum. Optimization with relaxed symmetry led to the SE(2+1) C_s structure in Figure 6b, which lies 590 meV below the cyclic neutral. The SOMOs of the D_{3h} and C_s SEs are shown beside the structures in Figure 6. The $\Delta\langle r^2\rangle$ values are 50 and 37 (a.u.)^2 for the D_{3h} and C_s SE respectively, and much smaller than in the two DBS anions.

4 Discussion

4.1 Implications for electron capture

Previous theoretical studies [36,39] have concentrated on the neutral cyclic species, which is the most stable form of HCl trimer. The present calculations demonstrate that Z- and Y-shaped forms will also be present. Free energies of formation and relative populations were not examined here. But the less rigid structures of these will enhance entropic contributions to their stability, and they are likely to represent significant fractions of the overall trimer population. This is important because there is no evidence for thermal electron attachment to the cyclic species, and the threshold for DA attachment is likely to be not far below that of the HCl monomer. The Z- and Y-shaped species are thus the ones most likely to be involved in DA processes. The CCSD(T) level results indicate that in principle both are capable of forming DBSs. However, in the Y species the barrier to DA lies below the ZPE of the neutral (Fig. 5) and dissociation should occur in a single vibration. A longer lifetime is possible in the case of the Z-shaped species, where the calculated DA threshold is at 0.06 eV (Fig. 3); but this low energy means that reaction (2) would occur with thermal energy electrons. Thus both are candidates for DA at thermal energies, and their presence could explain results seen in beam experiments and the irradiated gas.

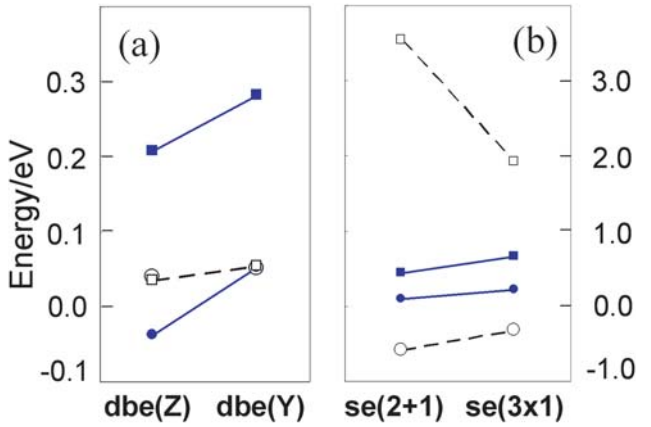

Fig. 7. Comparison of vertical detachment energy (□) and energy with respect to the cyclic neutral trimers (○) of different trimer anions of HF (filled symbols) and HCl (open symbols). HF data taken from reference [13].

The radiation chemical studies have given evidence for a second low energy capture process, which forms a long-lived negative ion intermediate. The most likely candidate for this is the $ClH^{\bullet}HCl^{-}$ SE, evidence for which was reported in reference [10]. In the ambient gas this may be clustered by one or more HCl molecules. As shown in Section 3 such a structure is exceedingly stable. Its formation must at some point involve bringing together HCl molecules with their dipoles opposed. This process will be explored elsewhere.

4.2 Comparison of HCl and HF species

Attention is now given to a comparison of the properties of the HCl trimer anions with those of the corresponding HF anions from reference [13], which is clearly of considerable interest. For this purpose it is convenient to use the energy of the cyclic neutral as the reference point for all HCl anions as was done in reference [13]. Following the terminology used there, the energy of either anion relative to this neutral is given by the equation:

$$E^A = E^N(G_A) - E^N(G_N) - VDE + E^0_{vib,A} - E^0_{vib,N}. \quad (5)$$

Here N = neutral, A = anion, and $E^N(G_X)$ represents the electronic energy of the neutral at the equilibrium geometry of X, $E^0_{vib,X}$ is the ZPE of X and VDE the vertical detachment energy. $E^N(G_A) - E^N(G_N)$ is the reorganization energy, E^N_{reorg}, for the neutral to take up the equilibrium geometry of the anion. The values of E^A and VDE for the four anions of the HF and HCl systems are compared in Figures 7a and 7b. The data for the HF species were taken from Figure 3 of reference [13].

The values of E^A are the negatives of the electron affinity with respect to the cyclic neutral. For the HCl SE(2+1) and SE(3×1) species those electron affinities are given in Table 1. Thus the E^A values are –0.327 and –0.590 eV, respectively. For the dbe(Z) and dbe(Y) species the EAs in Table 1 must be modified by the differences in ZPEs and binding energies of the Z and Y neutrals and the cyclic neutral (see Tabs. 1 and 3). The resulting E^As are 0.035 and 0.054 eV for dbe(Z) and dbe(Y), respectively, and both of these lie above cyclic neutral (Fig. 7a). This is also true for the dbe(Y) species of HF. However, the E^A for the dbe(Z) HF species is negative. The difference from the HCl dbe(Z) can be attributed to the fact that the dipole moment will be larger in the HF species.

Differences in geometry between an anion and neutral cause the VDE to increase above the EA. Thus large E^N_{reorg} values tend to be reflected in large VDEs. Reference to Figure 7a shows that the VDE values of the HF Z and Y species are significantly greater than those of the corresponding HCl species. This is largely due to the stronger binding in the HF neutral systems. For example the binding of the additional HX in going from dimer to cyclic trimer is ∼31 kJ mol^{-1} for HF versus ∼8.6 kJ mol^{-1} for HCl [39]. This contributes to E^N_{reorg} and hence causes the HF VDEs to be higher.

Reference to the results for the SE systems in Figure 7b indicates that the positions of HF and HCl species are reversed. The HCl anions now have the larger EAs (i.e. lie below the neutral) and have the larger VDE values. This is reminiscent of the effects observed in reference [16], were a comparison was made of the binding in linear $XH^{\bullet}HX^{-}$ structures for HF, HCl and HBr. The electron binding was found to increase with atomic number of the halogen. The excess electron entered into the σ^* orbital of the HCl and HBr systems, and this caused a marked extension in the HX bond lengths. This is not seen in HF systems, where the σ^* orbital is much higher in energy. The perturbation of the HCl structures in the SE(2+1) and SE(3×1) structures in Figure 6 is quite extensive. The HCl monomer MP2 bond length is 1.282 Å. The length in SE(3×1) is 1.435 Å. The perturbation is even greater in SE(2+1), where one of the opposing HCls is stretched to 1.709 Å. At the same time the $\Delta\langle r^2\rangle$ values are an order of magnitude smaller than those for the dbe(Z) and dbe(Y) species (Results, Sects. 2–4). Clearly the penetration into the σ^* orbital allows for very tight electron binding, and the bonding in these systems is significantly different from that in the HF species. Returning to Figure 7, the large VDEs values for the HCl SE systems are now seen to be due to the high E^N_{reorg} values, which arise from strong perturbations of the HCl bond lengths, and, especially in SE(2+1), the close proximity of the opposed hydrogens.

4.3 Summary

The present results confirm that the C_s Z- and Y-shaped $(HCl)_3$ neutral species are less stable than the C_{3h} cyclic species. However, they are the ones most likely to be involved in the capture of thermal electrons. Both are capable of forming DBS with electron affinities at the CCSD(T)//MP2 level of 16 and 43 meV for dbe(Z) and dbe(Y), respectively. However, the HCl dbe(Y) is expected to dissociate spontaneously to $H^{\bullet}+Cl^{-}(HCl)_{n-1}$. Although the electron is strongly bound in the D_{3h} HCl SE(3×1) anion (EA = 0.33 eV relative to the cyclic

neutral trimer), it is unstable and rearranges to a C_s $ClH{\cdot}ClH^{\bullet}HCl^{-}$ SE(2+1) species with an EA of 0.59 eV. The EAs of these two HCl SE species are much higher than those of their HF counterparts. A second important feature is that their H-halogen bond lengths are strongly perturbed.

The financial support of the Natural Sciences and Engineering Research Council of Canada and the University of Calgary is gratefully acknowledged. The authors are also indebted to Dr. Dake Yu, who carried out many of the preliminary calculations on this project and to Dr. Patrick Brunelle for assistance with the computer network and orbital contour plots.

References

1. D.C. Frost, C.A. McDowell, J. Chem. Phys. **29**, 503 (1958)
2. I.S. Buchel'nikova, Sov. Phys. JETP **35**, 783 (1959) [Zh. Eksperim. i Teor. Fiz. **35**, 1119 (1958)]
3. L.G. Christophorou, *Atomic and Molecular Radiation Physics* (Wiley, New York, 1971)
4. For earlier studies of these systems see, for example, references [5,6]
5. K. Rohr, J. Phys. B **10**, 1849 (1978)
6. R. Abouaf, D. Teillet-Billy, Chem. Phys. Lett. **73**, 106 (1980)
7. W. Domcke, Phys. Rep. **208**, 97 (1991).
8. M. Čízek, J. Horáček, W. Domcke, Phys. Rev. A **60**, 2873 (1999)
9. M. Čízek, J. Horáček, A.-Ch. Sergenton, D.B. Popoviæ, M. Allan, W. Domcke, T. Leininger, F.X. Gadea, Phys. Rev. A **63**, 62710 (2001)
10. H. Haberland, T. Richter, Z. Phys. D **10**, 99 (1988)
11. J.H. Hendricks, H.L. de Clercq, S.A. Lyapustina, K.H. Bowen, J. Chem. Phys. **107**, 2962 (1997)
12. M. Gutowski, P. Skurski, J. Chem. Phys. **107**, 2962 (1997)
13. M. Gutowski, C.S. Hall, L. Adamowicz, J.H. Hendricks, H.L. de Clercq, S.A. Lyapustina, J.M. Niles, S.-J. Xu, K.H. Bowen, Phys. Rev. Lett. **88**, 143001 (2002)
14. X.Y. Hao, Z.-R. Li, D. Wu, Y. Wang, Ze.-S. Li, C.-C. Sun, J. Chem. Phys. **118**, 83 (2003)
15. M. Gutowski, P. Skurski, J. Phys. Chem. B **101**, 9143 (1997)
16. A. Rauk, D.A. Armstrong, J. Phys. Chem. A **106**, 400 (2002)
17. K. Imura, T. Kasai, H. Ohoyama, H. Takahashi, R. Naaman, Chem. Phys. Lett. **259**, 356 (1996)
18. C. Desfrançois, H. Abdoul-Carime, N. Khelifa, J.P. Scherman, Phys. Rev. Lett. **73**, 2436 (1994); and references cited therein
19. C. Sarasola, J.E. Fowler, J.M. Ugalde, J. Chem. Phys. **110**, 11717 (1999)
20. A. Rauk, D.A. Armstrong, Int. J. Quant. Chem. **95**, 683 (2003); A. Rauk, D.A. Armstrong, Int. J. Quant. Chem. **96**, 69 (2004)
21. R.S. Davidow, D.A. Armstrong, J. Chem. Phys. **48**, 1235 (1968)
22. G.R.A. Johnson, J.L. Redpath, J. Phys. Chem. **72**, 765 (1968)
23. G.R.A. Johnson, J.L. Redpath, Trans. Faraday Soc. **66**, 861(1970)
24. S.S. Nagra, D.A. Armstrong, Can. J. Chem. **54**, 3580 (1976)
25. J.H. Pendergrass, L.A. Booth, F.T. Finch, T.G. Frank, Altern. Energy Syst. **2**, 2671 (1981)
26. A. Rauk, D.A. Armstrong, J. Phys. Chem. A **104**, 7651 (2000)
27. S.S. Nagra, D.A. Armstrong, Can. J. Chem. **54**, 3580 (1976)
28. I. Szamrej, M. Foryś, W. Tchórzewska, Radiat. Phys. Chem., **38**, 547 (1991)
29. E.L. Quitevis, K.H. Bowen, G.W. Liesegange, D.R. Herschbach, J. Phys. Chem. **87**, 2076 (1983)
30. . T. Speck, J.-L. Le Garrec, S. Le Picard, A. Canosa, J.B.A. Mitchell, B.R. Rowe, J. Chem. Phys. **114**, 8303 (2001)
31. M.J. Frisch, G.W. Trucks, H.B. Schlegel, G.E. Scuseria, M.A. Robb, J.R. Cheeseman, V.G. Zakrzewski, J.A. Montgomery Jr, R.E. Stratmann, J.C. Burant, S. Dapprich, J.M. Millam, A.D. Daniels, K.N. Kudin, M.C. Strain, O. Farkas, J. Tomasi, V. Barone, M. Cossi, R. Cammi, B. Mennucci, C. Pomelli, C. Adamo, S. Clifford, J. Ochterski, G.A. Petersson, P.Y. Ayala, Q. Cui, K. Morokuma, P. Salvador, J.J. Dannenberg, D.K. Malick, A.D. Rabuck, K. Raghavachari, J.B. Foresman, J. Cioslowski, J.V. Ortiz, A.G. Baboul, B.B. Stefanov, G. Liu, A. Liashenko, P. Piskorz, I. Komaromi, R. Gomperts, R.L. Martin, D.J. Fox, T. Keith, M.A. Al-Laham, C.Y. Peng, A. Nanayakkara, M. Challacombe, P.M. W. Gill, B. Johnson, W. Chen, M.W. Wong, J.L. Andres, C. Gonzalez, M. Head-Gordon, E.S. Replogle, J.A. Pople, Gaussian 98, Revision A.11, Gaussian, Inc., Pittsburgh PA, 2001
32. M.J. Frisch, G.W. Trucks, H.B. Schlegel, G.E. Scuseria, M.A. Robb, J.R. Cheeseman, J.A. Montgomery Jr, T. Vreven, K.N. Kudin, J.C. Burant, J.M. Millam, S.S. Iyengar, J. Tomasi, V. Barone, B. Mennucci, M. Cossi, G. Scalmani, N. Rega, G.A. Petersson, H. Nakatsuji, M. Hada, M. Ehara, K. Toyota, R. Fukuda, J. Hasegawa, M. Ishida, T. Nakajima, Y. Honda, O. Kitao, H. Nakai, M. Klene, X. Li, J.E. Knox, H.P. Hratchian, J.B. Cross, C. Adamo, J. Jaramillo, R. Gomperts, R. E. Stratmann, O. Yazyev, A.J. Austin, R. Cammi, C. Pomelli, J.W. Ochterski, P.Y. Ayala, K. Morokuma, G.A. Voth, P. Salvador, J.J. Dannenberg, V.G. Zakrzewski, S. Dapprich, A.D. Daniels, M.C. Strain, O. Farkas, D.K. Malick, A.D. Rabuck, K. Raghavachari, J.B. Foresman, J.V. Ortiz, Q. Cui, A.G. Baboul, S. Clifford, J. Cioslowski, B.B. Stefanov, G. Liu, A. Liashenko, P. Piskorz, I. Komaromi, R.L. Martin, D.J. Fox, T. Keith, M.A. Al-Laham, C.Y. Peng, A. Nanayakkara, M. Challacombe, P.M.W. Gill, B. Johnson, W. Chen, M.W. Wong, C. Gonzalez, J.A. Pople, Gaussian 03, Revision B.05, Gaussian, Inc., Pittsburgh PA, 2003
33. A.P. Scott, L. Radom, J. Phys. Chem. **100**, 16502 (1996)
34. R.J. Bartlett, J.F. Stanton, in *Reviews in Comparative computational Chemistry*, edited by K.B. Lipkowitz, D.B. Boyd (VCH Publishers, Inc., New York, 1994), Vol. V
35. K.A. Peterson, T. H. Dunning, J. Chem. Phys. **102**, 2032 (1995)
36. Z. Latajka, S. Scheiner, Chem. Phys. **216**, 37 (1997)
37. M. Fárník, S. Davis, D.J. Nesbitt, Faraday Disc. **118**, 63 (2001).
38. M. Fárník, D.J. Nesbitt, J. Chem. Phys. **121**, 12386 (2004).
39. R.C. Guedes, P.C. do Couto, B.J. Costa Cabral, J. Chem. Phys. **118**, 1272 (2003)